EVALUATION OF WITHDRAWAL STRENGTH OF SELF-TAPPING SCREW INSERTED INTO CROSS-LAMINATED TIMBER WITH DIFFERENT ANATOMICAL ASPECTS

Sarah Amira

Doctoral Student
Department of Bioresource Sciences
United Graduate School of Agricultural Science
Gifu University (placement at Shizuoka University)
836 Ohya, Suruga Ward, Shizuoka 422-8529, Japan
E-mail: sarah.amira.19@shizuoka.ac.jp

*Kenji Kobayashi**

Associate Professor
E-mail: kobayashi.kenji.b@shizuoka.ac.jp

Keita Ogawa

Assistant Professor
Department of Bioresource Sciences
Faculty of Agriculture
Shizuoka University
836 Ohya, Suruga Ward, Shizuoka 422-8529, Japan
E-mail: ogawa.keita@shizuoka.ac.jp

(Received September 2023)

Abstract. The use of cross-laminated timber (CLT) technology is witnessing an upsurge in Japan because of its satisfactory performance under seismic conditions. The withdrawal strength (f_{ax}) of a single self-tapping screw (STS) inserted into the CLT was observed using a withdrawal test. The experimental results showed that f_{ax} of the partially threaded STS was higher than that of the fully threaded STS when inserted perpendicular to the grain. The empirical model used to predict f_{ax} provided in the European standard for the design of timber structures was evaluated by comparing the predicted values with the experimental results, which showed that the empirical model was only suitable for predicting the withdrawal strength of specimens with STSs inserted perpendicular to the grain. Therefore, a new probabilistic model was proposed for specimens inserted with STSs inserted parallel to the grain. The failure modes with respect to the orthotropic anatomy of wood materials were observed.

Keywords: Withdrawal strength, probabilistic model, failure mode.

INTRODUCTION

Timber construction techniques have been used to construct temples and shrines in Japan since ancient times. Most residential houses in Japan are constructed using wood. Cross-laminated timber (CLT) is an engineered wood product used in wooden houses to achieve environmental sustainability in Europe, Australia, and North America. Interest in CLT as a newly developed technology has increased in Japan. Izzi et al (2018) stated that CLT structures exhibit satisfactory performance under seismic conditions because of the high strength-to-weight ratio and in-plane stiffness of the CLT panels and the capacity of connections to resist loads with ductile deformations and limited strength impairment.

Self-tapping screws (STSs) optimized mainly for axial load represent a state-of-the-art fastening and reinforcement technique in CLT construction. STSs are highly recommended by CLT manufacturers and designers, both overseas and in Japan, owing to their economic benefits and easy handling (Mohammad et al 2013; Dietsch and Brandner 2015; Kobayashi 2015). Recently, the Japanese

* Corresponding author

Industrial Standard for STSs for timber joints (JIS A 1503) has been published. However, this standard does not include withdrawal strength and head pull-through properties because their inclusion requires the consideration of the properties of the adjacent wood; the JIS is primarily focused on the fastener property (Goto et al 2018). CLT buildings are primarily constructed for residential use and restricted to three stories because of the limited local wood sources, which results in costly and unaffordable CLT production (Passarelli and Koshihara 2018). The lack of standards for CLT structures in Japan renders it difficult to assess the mechanical strength of wood panels and the capacity of connectors to resist loads. An analytical approach for CLT connections is necessary to precisely design CLT constructions and reduce the excessive use of wood in the future.

The raw material for CLT structures should be potentially sourced from species that are readily available in sufficient quantities. Indonesia, in Southeast Asia, has a topography similar to that of Japan and faces the common problem of being an earthquake-prone area. Southeast Asia has one of the oldest tropical forests in the world and supplies large volumes of wood-based products to the world (Okuda et al 2018). The growth of trees as the source of raw wood materials from the tropical natural forest, particularly trees of large diameter with high-quality wood, took a long time to be harvested, one that has seen reckless exploitation in the past. In response to this challenge, Indonesia has planted fast-growing tree species to reduce the use of natural forest trees. Some plantation species in the tropics may grow faster than those in temperate climates because of year-round sunlight exposure. Fast-growing plantation species, such as jabon (*Neolamarckia cadamba* (Roxb.) Bosser), show a relatively high mean annual increment, with a growth of 7-10 cm/yr in diameter and 3-6 m/yr in height within 5 yr (Mansur and Tuheteru 2010).

Neolamarckia cadamba, commonly known in English as bur flower-tree and locally known as kadam or jabon, demonstrates high prospects for industrial plantations and reforestation plants in Indonesia. This species is also expected to become increasingly important for the timber industry in the future, particularly when woodworking raw materials from natural forests are estimated to decrease in the coming years (Krisnawati et al 2011). The wood from this species is typically easy to work on with hand and machine tools. It can be easily resawed, crosscut, and honed and the honed surface produced is smooth. However, its use is mostly limited to furniture, plywood, pulps, and chips, and it is not yet a major structural timber component in the construction sector (Okuda et al 2018). Moreover, CLT reference standards for wood species properties and connections performance are lacking. To ascertain the prospects of this species for CLT construction, its properties are supposed to be investigated against those of several common commercial species used as CLT materials.

The connection geometry, which mainly influences the fastener behavior, includes the axial strengths of the fastener, the density of the wood in which it is inserted, and the direction of loading with respect to the grain orientation (Mahdavifar et al 2018). Previously, studies were conducted on the withdrawal capacity of an STS in a single layer and CLT using a probabilistic approach covering the entire density and diameter bandwidths (Ringhofer et al 2015; Brandner et al 2018; Brandner 2019). However, the length of the inserted STS threaded part was not considered.

The present study investigates the withdrawal performance of the STSs inserted into a CLT with respect to the density of the timber species, the effective insertion length of the STS threaded part, and the CLT side with the STS insertion. The experimental results were evaluated using the authorized prediction equation in EN 1995-1-1:2004/A1 (2008), and a probabilistic model approach was proposed. Moreover, the types of failures that occurred in the withdrawal test were also observed.

MATERIALS AND METHODS

Materials

The withdrawal strength of a single STS inserted into a CLT was measured using a withdrawal-loaded test. The test materials used in this study

were composed of small pieces of CLT and glue-laminated timber (GLT) with two types of STSs (fully threaded and partially threaded). Jabon (*Neolamarckia cadamba* (Roxb.)), sourced from Medan, Indonesia, was used as a representative Indonesian fast-growing hardwood. Sugi (*Cryptomeria japonica* D. Don), hinoki (*Chamaecyparis obtusa*), and karamatsu (*Larix kaempferi*) wood species were used as the representative commercial Japanese softwood samples.

Lamina selection is a prerequisite of the CLT manufacturing process that prevents defects and substandard quality in the final product. Once the lamina materials were visually selected to prevent knots, decay, and finger joints (on jabon materials), they were classified physically and mechanically. The lamina density ρ (kg/m^3) was calculated using the gravimetry method, as depicted in Eq 1.

$$\rho = \frac{m}{V}, \tag{1}$$

where m is the lamina mass (kg) and V is the lamina volume (m^3). The lamina materials were selected according to the Japanese Agricultural Standard for CLT (JAS 3079-2013) by determining the grade of their Young's moduli of bending. Static bending tests were conducted according to JIS Z 2101 (2009), and the Young's modulus of bending E_b (GPa) was calculated using the following expressions:

$$E_b = \frac{l^3 \Delta P}{48 I \Delta y}, \tag{2}$$

$$I = \frac{bh^3}{12}, \tag{3}$$

where l is the bending span (mm), I is the moment inertia of area (mm^4), ΔP is the change in load in the proportional limit area (kN), Δy is the deflection at the center of the span corresponding to ΔP (mm), b is the width of the cross section (mm), and h is the thickness (mm). $\Delta P/\Delta y$ is the slope of load and deflection changes in the elastic range.

The obtained mean Young's modulus of the jabon lamina was 6.614 GPa, with minimum and maximum values of 2.516 and 16.034 GPa, respectively. Therefore, according to JAS 3079-2013, jabon laminas were classified into the M 30A ($E_b \geq 2.5$ GPa) to M 60A grades ($E_b \geq 5$ GPa), which satisfied the minimum grade for structural purposes as CLT materials. Sugi laminas are classified into the M 60A to M 120A ($E_b \geq 10$ GPa) grades, whereas hinoki and karamatsu laminas are classified into the M 90A ($E_b \geq 7.5$ GPa) to M 120A grades. Lamina grading is used as a reference for CLT assembly configuration. Laminas with lower grades were configured for the inner layers, and the higher-graded laminas were configured for the outer layers in this study.

The test specimens were manufactured as five-layer CLT and GLT, yielding an approach model for solid wood. The laminas were adhered to using the aqueous polymer isocyanate (API) adhesive TP-111 at a ratio of 100:15 to a cross-linking agent. The glue spread rate was 250 g/m^2, with a double glue line for face and edge bonding. Using a compressive machine, the assemblies were adjusted with pressures of 1 MPa and retained under pressure at 20°C for 30 min. The API-bonded specimens were produced and conditioned at 65 ± 5% RH and 20 ± 2°C for 2 wk to reach a MC close to 12%.

Three parts of the CLT were available for STS insertion: A, the outermost surface of the CLT; B, parallel to the grain of the CLT core layer; and C, perpendicular to the grain of the CLT core layer. Type A was composed of five layers, whereas types B and C were composed of three layers as the expected effective layers. Ten replicates were used for each combination series. The design of specimen dimensions and STS insertion points are shown in Fig 1. The insertion point of the STS on the CLT was determined according to the European standards for the design of timber structures (EN 1995-1-1 2004 and EN 1995-1-1:2004/A1 2008). Two types of connector, fully threaded STS (PX8-260) and partially threaded STS (PS8-260), manufactured by Synegic Co., Ltd., with a thread diameter of 8 mm and total length L of 260 mm, as illustrated in Fig 2, were considered and distinguished by the effective length of the STS threaded part inserted into the specimen (the shapes of the screw head and screw tip

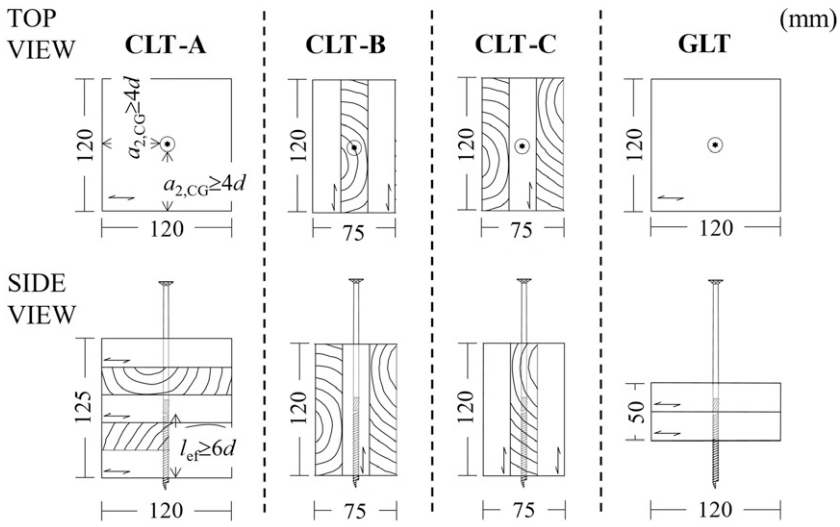

Figure 1. The design of specimen dimensions and self-tapping screw insertion point.

were ignored). The nomenclature of the specimens includes the first letter of the wood species (S for sugi, J for jabon, H for hinoki, and K for karamatsu), followed by the first letter of the STS type (P for partially threaded STS and F for fully threaded STS), and the last character indicating the type of specimen and its STS insertion point (GLT, CLT-A, CLT-B, and CLT-C). Table 1 lists the mean values of the lamina material density (ρ) and the effective length of the fully threaded STS (l_{ef}) for each series.

Withdrawal Test

The STS was driven through the entire test specimen to avoid the tip influencing the layer orientation, as shown in Fig 1. A turned washer with a diameter of 8 mm was used to fix the screw head to the screw grip. A screw grip shaped to fit the head of the STS was attached to the load head of a universal testing machine (UTM) (AG-I 250 kN; Shimadzu Co.). Two displacement gauges (CDP-25) with a capacity of 25 mm (manufactured

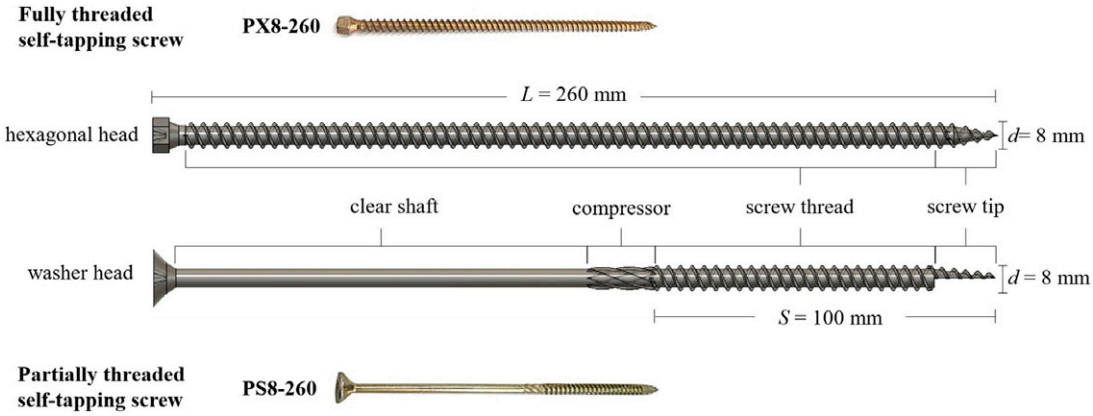

Figure 2. Connector properties: fully threaded self-tapping screw (above) and partially threaded self-tapping screw (below).

Table 1. The mean value of lamina density (ρ) and effective insertion length of self-tapping screw threaded part (l_{ef}) for each series.

	n	ρ		l_{ef}	
Series	#	Mean (kg/m^3)	CoV (%)	Mean (mm)	CoV (%)
S.P.GLT	10	366.7	5.8	32	—
S.P.CLT-A	10	349.2	2.9	80	—
S.P.CLT-B	10	373.0	2.8	80	—
S.P.CLT-C	10	367.3	2.5	80	—
S.F.GLT	10	369.9	4.8	50.9	0.2
S.F.CLT-A	10	376.9	5.7	127.1	0.2
S.F.CLT-B	10	372.4	2.8	120.4	0.7
S.F.CLT-C	10	363.0	5.3	120.3	1.1
J.P.GLT	10	402.7	2.3	32	—
J.P.CLT-A	10	448.3	3.6	80	—
J.P.CLT-B	10	411.5	4.2	80	—
J.P.CLT-C	10	410.4	3.5	80	—
J.F.GLT	10	425.3	7.5	49.5	0.1
J.F.CLT-A	10	426.7	2.9	123.7	0.1
J.F.CLT-B	10	414.2	4.8	118.3	1.4
J.F.CLT-C	10	411.1	3.9	121.5	0.4
H.P.GLT	10	409.2	2.0	32	—
H.P.CLT-A	10	432.6	3.8	80	—
H.P.CLT-B	10	439.2	4.0	80	—
H.P.CLT-C	10	473.9	5.1	80	—
H.F.GLT	10	409.6	2.0	50.8	0.2
H.F.CLT-A	10	432.8	2.2	126.7	1.7
H.F.CLT-B	10	455.7	2.1	120.3	0.4
H.F.CLT-C	10	448.7	2.2	118.9	0.5
K.P.GLT	10	515.3	5.2	32	—
K.P.CLT-A	10	524.4	1.4	80	—
K.P.CLT-B	10	524.5	2.5	80	—
K.P.CLT-C	10	525.9	2.2	80	—
K.F.GLT	10	548.3	4.0	50.5	5.2
K.F.CLT-A	10	530.6	4.4	126.0	2.5
K.F.CLT-B	10	541.7	2.8	120.8	0.3
K.F.CLT-C	10	539.2	1.2	120.4	0.3

by the Tokyo Instrument Research Institute) were attached to record the displacement during the withdrawal test. The withdrawal test apparatus is illustrated in Fig 3.

Monotonic static loading was performed at a constant rate of 1 mm/min. The maximum load, F_{max} was determined, and the f_{ax} (N/mm^2) was calculated using the following equation (Ringhofer et al 2015; Brandner 2019) according to EN 1382 (1999)

$$f_{ax} = \frac{F_{max}}{d\pi l_{ef}}, \tag{4}$$

where F_{max} is the maximum load attained in each test (N), d is the thread diameter (mm), and l_{ef} is the effective insertion length of the threaded part (mm).

According to EN 1995-1-1:2004/A1 (2008), the characteristic withdrawal strength of a single screw $f_{ax,EC5}$ (N/mm^2) is calculated as follows:

$$f_{ax,\ EC5} = 0.52 d^{-0.5} {l_{ef}}^{-0.1} \rho^{0.8}, \tag{5}$$

where d is the thread diameter (mm), l_{ef} is the effective insertion length of the threaded part of the STS (mm), and ρ is the density (kg/m^3). This equation should be divided by π such that the result can be compared with the experimental value obtained from Eq 4. Thus, a comparative equation is generated as follows:

$$f_{ax,\ EC5}/\pi = \frac{0.52 d^{-0.5} {l_{ef}}^{-0.1} \rho_k^{0.8}}{\pi}, \tag{6}$$

Furthermore, the lower 5%-quantile value, assuming a normal distribution of the experimental results, was calculated using the following equation.

$$5\%-\text{quantile value} = \overline{x}(1 - kCV), \tag{7}$$

where $\overline{x}$ is the mean value; k is the coefficient for obtaining the 95% lower tolerance limit at the 75% confidence level, which is 2.104 for 10 specimens of each series (AIJ, 2006); and CV denotes the coefficient of variation, obtained from the ratio of the standard deviation to the mean value.

RESULTS AND DISCUSSION

Relationship between Withdrawal Load and Displacement

The differences in f_{ax} for each specimen series are shown in Fig 4, and the average value is listed in Table 2. The lowest average f_{ax} was obtained for the partially threaded STS on the jabon CLT-B specimen with a value of 3.4 N/mm^2, and the highest average value was obtained from the partially threaded STS on the karamatsu CLT-A specimen (9.15 N/mm^2). The f_{ax} values of the partially threaded STSs were higher than those of the fully threaded STSs for the CLT-A, CLT-C, and

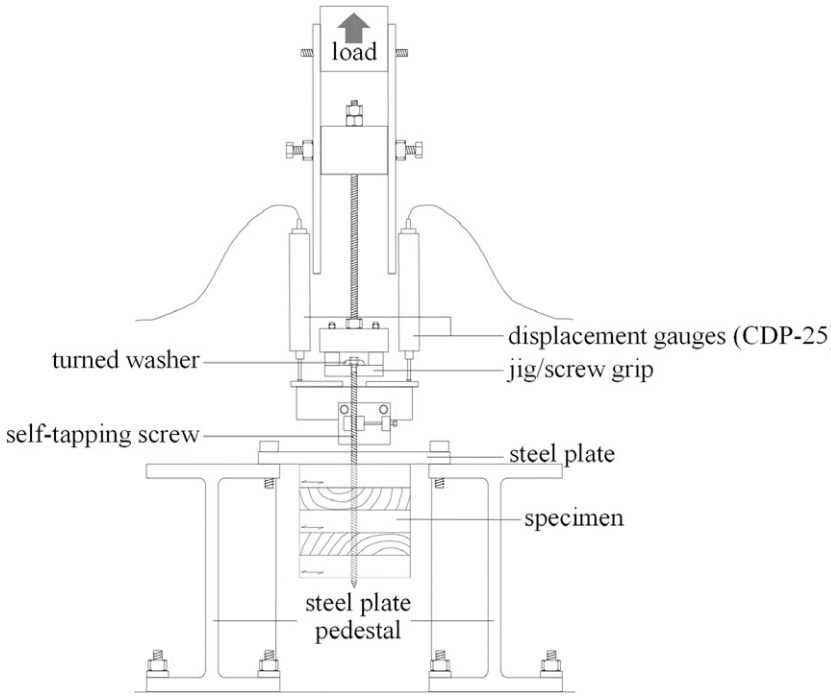

Figure 3. Withdrawal test apparatus.

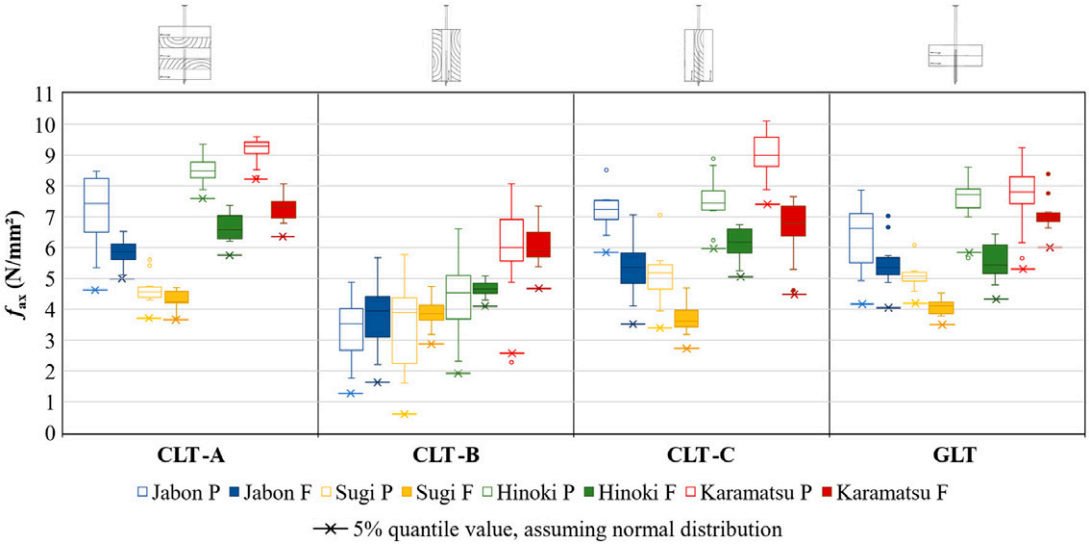

Figure 4. Boxplot of withdrawal strength regarding the lamina species, effective insertion length of self-tapping screw threaded part, and insertion points.

Table 2. The mean value of F_{ax} and f_{ax} for each series.

	n	F_{max}		f_{ax}	
Series	#	Mean (kN)	CoV (%)	mean (N/mm^2)	CoV (%)
S.P.GLT	10	4.09	8.15	5.09	8.15
S.P.CLT-A	10	9.44	9.69	4.70	9.69
S.P.CLT-B	10	7.04	38.83	3.50	38.83
S.P.CLT-C	10	10.42	16.11	5.18	16.11
S.F.GLT	10	5.24	6.69	4.10	6.66
S.F.CLT-A	10	13.79	6.90	4.32	6.84
S.F.CLT-B	10	11.82	12.24	3.91	12.14
S.F.CLT-C	10	11.29	12.47	3.74	12.43
J.P.GLT	10	5.15	16.44	6.41	16.44
J.P.CLT-A	10	14.44	16.80	7.18	16.80
J.P.CLT-B	10	6.84	29.15	3.40	29.15
J.P.CLT-C	10	14.79	9.69	7.36	9.69
J.F.GLT	10	6.94	12.84	5.58	12.82
J.F.CLT-A	10	18.20	6.91	5.85	6.83
J.F.CLT-B	10	11.35	27.29	3.82	26.73
J.F.CLT-C	10	16.39	16.01	5.37	16.10
H.P.GLT	10	6.06	10.62	7.54	10.62
H.P.CLT-A	10	17.13	5.16	8.52	5.16
H.P.CLT-B	10	8.95	26.57	4.45	26.57
H.P.CLT-C	9	15.25	10.04	7.59	10.04
H.F.GLT	10	7.13	10.59	5.59	10.56
H.F.CLT-A	10	21.23	6.01	6.67	6.45
H.F.CLT-B	10	14.15	5.80	4.68	5.64
H.F.CLT-C	10	18.37	8.22	6.15	8.34
K.P.GLT	10	6.19	14.69	7.70	14.69
K.P.CLT-A	10	18.39	4.82	9.15	4.82
K.P.CLT-B	10	11.90	26.58	5.92	26.58
K.P.CLT-C	10	18.07	8.18	8.99	8.18
K.F.GLT	10	9.06	7.73	7.14	7.49
K.F.CLT-A	10	23.18	5.06	7.33	6.21
K.F.CLT-B	10	18.69	11.17	6.16	11.30
K.F.CLT-C	10	19.97	15.13	6.60	15.14

GLT specimens. However, the differences were found less significant for the CLT-B specimens. Within a uniform thread diameter, when the withdrawal load is applied perpendicular to the grain, the shorter the l_{ef}, the smaller the f_{ax}, which is a consequence of the divisor variable in Eq 4. Claus et al (2022) investigated the force distribution along the STSs using fiber Bragg grating measurements and found that the force distribution on an STS insertion of length 270 mm into a GLT material was relatively constant when the screw axis to the grain angle was 0°. When the screw axis to the grain angle was 90°, the withdrawal force tended to be higher at the uppermost screw thread, which then gradually decreased to the lower end of the inserted screw thread. In other words, the length of the inserted threaded part of the STS did not significantly affect the withdrawal force when it was inserted parallel to the grain.

Similar patterns were observed in the CLT-A, CLT-C, and GLT specimens when the angle between the STS axis and wood grain was 90°. However, the withdrawal load was applied in the radial direction of the wood in the CLT-A and GLT specimens, whereas in the CLT-C specimens, the withdrawal load was applied in the tangential direction of the adjacent wood, which in some way altered the difference to the failure occurrences, as discussed later.

Evaluation of the Prediction Model of Withdrawal Strength

The characteristic withdrawal strength of a single screw in EN 1995-1-1:2004/A1 (2008) is basically described by the characteristic density values for European solid timber (EN 338, 2016) and GLT provided in the Eurocode standards (EN 1194, 1999). For the materials used in this study, the withdrawal strength values were to be evaluated for each specimen, along with the mean and 5%-quantile of the experimental series results to the predicted value calculated by Eq 6.

Significant correlations between the experimental results and predicted values are found for GLT, CLT-A, and CLT-C when each specimen within the series is analyzed, as shown in Fig 5. The wide range of density distributions in the experimental results disintegrates the withdrawal strength values predicted using Eq 6. When the mean values are projected onto both the experimental results and predicted values obtained using Eq 6, as shown in Fig 6, a significant correlation is noted for each specimen within the series. Figure 7 shows a comparison of the 5% quantile values of the experimental results and those predicted using Eq 6. Significant correlations can be observed for the GLT and CLT-A specimens; however, the correlations diminish in the remaining specimens. The values predicted using the empirical model in EN 1995-1-1:2004/A1 (2008), except for CLT-B

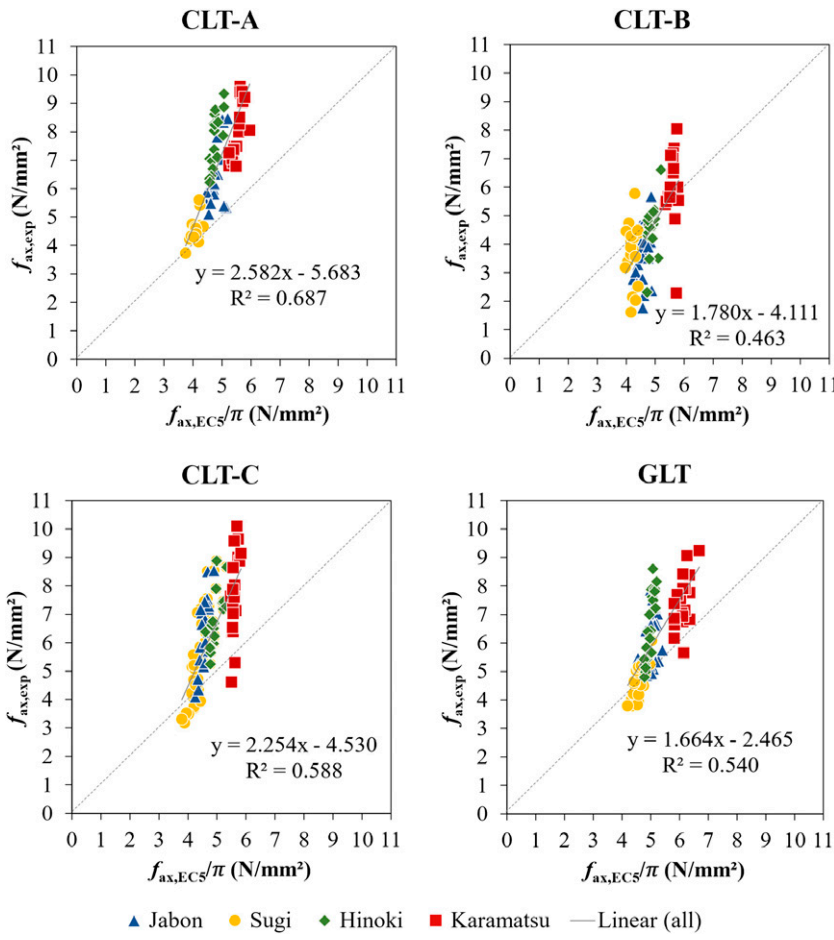

Figure 5. The comparison of experimental results and predicted values by Eq 6.

specimens, did not overestimate the experimental results, which was the expected anticipation for structural designing. Based on the comparison of the values predicted using the empirical model in EN 1995-1-1:2004/A1 (2008) with the calculated experimental values, it can be deduced that the empirical model (Eq 6) is only suitable for the specimens with STSs perpendicular to the grain (90°) if each specimen and 5%-quantile values are considered.

Even though the low withdrawal strength values of STSs inserted parallel to the grain (CLT-B) from experimental results implicitly remind us that the installation of STS in the narrow edge parallel to the grain is recommended to be avoided (Uibel and Blaß 2013), the author proposed the new probabilistic model approach for CLT-B specimens for the anticipatory step in any circumstances. The relationship between f_{ax} and density is usually described by a power regression model of the form $f_{ax} = a\rho^b\varepsilon$, where a and b are the regression parameters, with a as the scaling parameter and b as the power parameter, and ε is the error/randomness in the regression model (Brandner 2019). According to Eq 5 in EN 1995-1-1:2004/A1 (2008), the effective insertion length of the STS threaded part, l_{ef} is also described by a power model. Therefore, the predicted withdrawal strength regarding the wood density and effective insertion length of STS was described in the following form, with a as the scaling parameter and b and c as the power parameters.

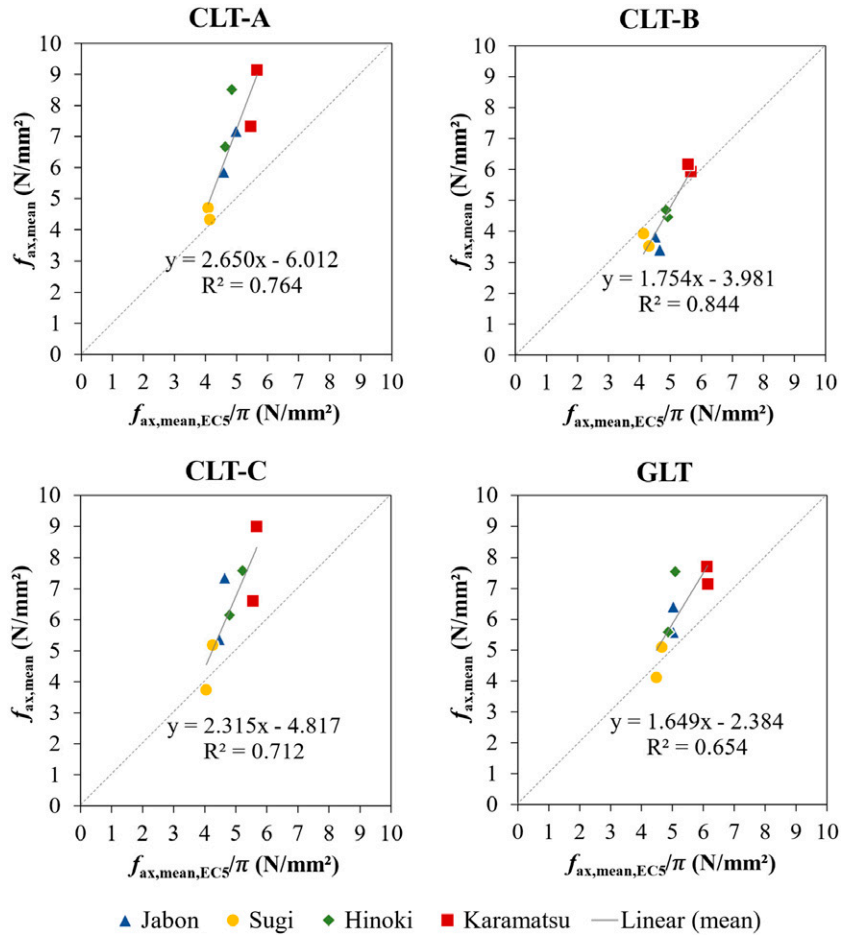

Figure 6. The comparison of mean experimental results and predicted values by Eq 6.

$$f_{ax,\,pred} = a\rho^{b} l_{ef}{}^{c} \tag{8}$$

The substitution variables for the equation above were obtained to make the sum of quadratic differences between the whole experimental results and the proposed prediction model at the minimum. Therefore, the new prediction model for CLT-B specimens with the uniform STS thread diameter at 8 mm was reformed as follows. This proposed model included the π division factor in the equation.

$$f_{ax,\,pred} = 0.0002 l_{ef}{}^{0.08} \rho^{1.6} \tag{9}$$

The proposed prediction model for CLT-B was evaluated by linear regressive analysis with each specimen, mean, and 5%-quantile values of the experimental series results as projected in Fig 8(a), (b), and (c), respectively. When the overall values of the experimental results and the predicted values calculated from the proposed Eq 9 were compared, the linearity was obtained. A more significant linearity was found if the mean withdrawal strength of each series was compared. The 5%-quantile of predicted values from the proposed model in Eq 9 overestimated the 5%-quantile values of experimental results at the near-threshold significance level within the limited parameters in this study. There might also be other wood anatomical parameters that possibly have an influence on the withdrawal strength (Brandner 2019).

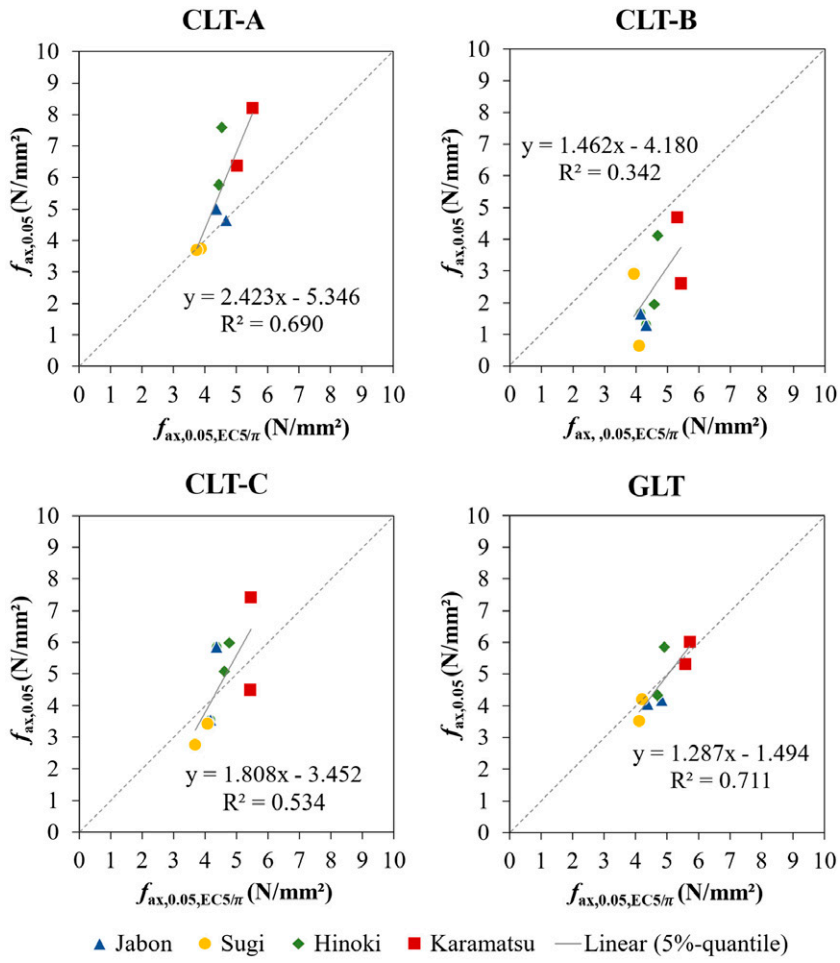

Figure 7. The comparison of 5%-quantile experimental results and predicted values by Eq 6.

However, the projected ρ values to both Eqs 6 and 9 generated a disproportionate distribution on $f_{ax,EC5}/\pi$ and $f_{ax,pred}$ of CLT-B and CLT-C. This is possibly the causative effect of the unspecific value of ρ, which is the mean value of the density of the whole lamina used for CLT layers instead of the STS-adjacent CLT layer density.

Influence of Parameters to Withdrawal Strength

Density, ρ, was the only wood characteristic that considerably influenced the withdrawal strength in this study, and the effective insertion length of the STS threaded part, l_{ef}, was the representative geometrical aspect of STS. Within the limited range of the above parameters, the significance of influencing the withdrawal strength of STS was analyzed through linear regression indicated by the coefficient of determination, R^2. As shown in Fig 9, the significant influence of lamina density within species on the withdrawal strength was indicated by the surrounded regression equations that were found on S.F.CLT-A, S.F.CLT-C, H.F.GLT, H.F.CLT-A, H.F.CLT-B, K.F.CLT-A, S.P.GLT, and S.P.CLT-A. None of the jabon specimens showed a significant effect of the density on the withdrawal strength. Brandner (2019) found out that the withdrawal strength of screws inserted in hardwood increased disharmonious

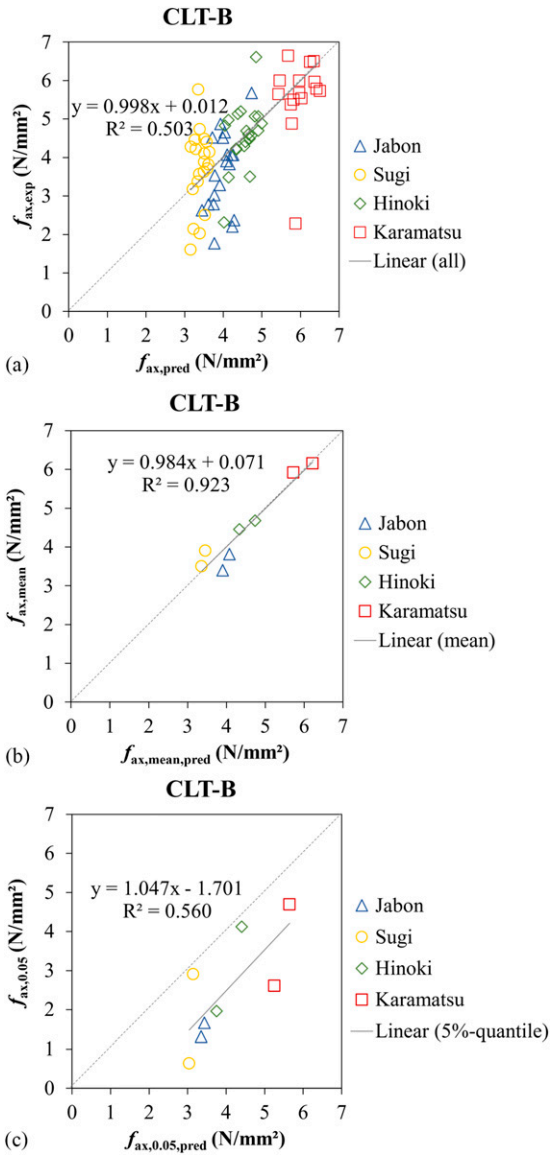

Figure 8. Correlation of the experimental results and the proposed predicted values by Eq 9: (a) each specimen values, (b) mean values, and (c) 5%-quantile values.

with increasing density, which was not the case in softwood (Uibel and Blaß 2007).

Regarding the two types of STS used in this study, the effective insertion length of the STS threaded part affects the withdrawal strength significantly negative on sugi and hinoki GLT, hinoki and karamatsu CLT-A, and a whole specimen of CLT-C (Fig 10). This negative effect of l_{ef} is also reasonably interpreted by the power value in the empirical model, Eq 5.

Failure Modes

Regarding the angle between the STS axis as well as the withdrawal load direction and the grain direction, they were grouped into 0° and 90°. The CLT-B specimen was the only specimen configuration, which is inserted by the STS parallel to the grain (0°). The CLT-A, CLT-C, and GLT were technically in the same state, which is inserted by the STS perpendicular to the grain (90°). However, the difference was noticed in the orthotropic anatomy of the wood materials. The STS was inserted in the radial direction through the crossed layups configuration in the CLT-A specimen. In unidirectional layups, the STS insertion was subjected to GLT in the same direction as CLT-A. And the direction of the STS insertion to the CLT-C was tangential. According to the mentioned conditions, the typical forms of failure modes were observed.

In this study, the failure modes were distinguished into three categories. First, the withdrawal failure, which is an initial failure in the withdrawal test, was characterized by the shear failure at the wooden members surrounding the STS to the sticking out of the upmost layer of CLT around the STS (Pang et al 2020), depicted in Fig 11. The second failure mode was a crack perpendicular to the withdrawal test direction (Fig 12), and the third failure mode was split as the further impact of the crack represented in Fig 13 was categorized into severe damages.

The withdrawal failures were found all over the series before the continued damage occurred. The crack failures occurred on one specimen of H.F.CLT-C, six K.F.CLT-C, seven K.P.CLT-C, one K.F.GLT, and two K.P.GLT. Four K.F.CLT-C, one K.P.CLT-C, and one K.F.GLT were found with split failure. The severe failures, cracks, and splits mostly occurred on the dense specimens in the tangential direction of the withdrawal force. A similar failure also occurred in the previous study by Xu et al (2021), with splitting and tension cracks

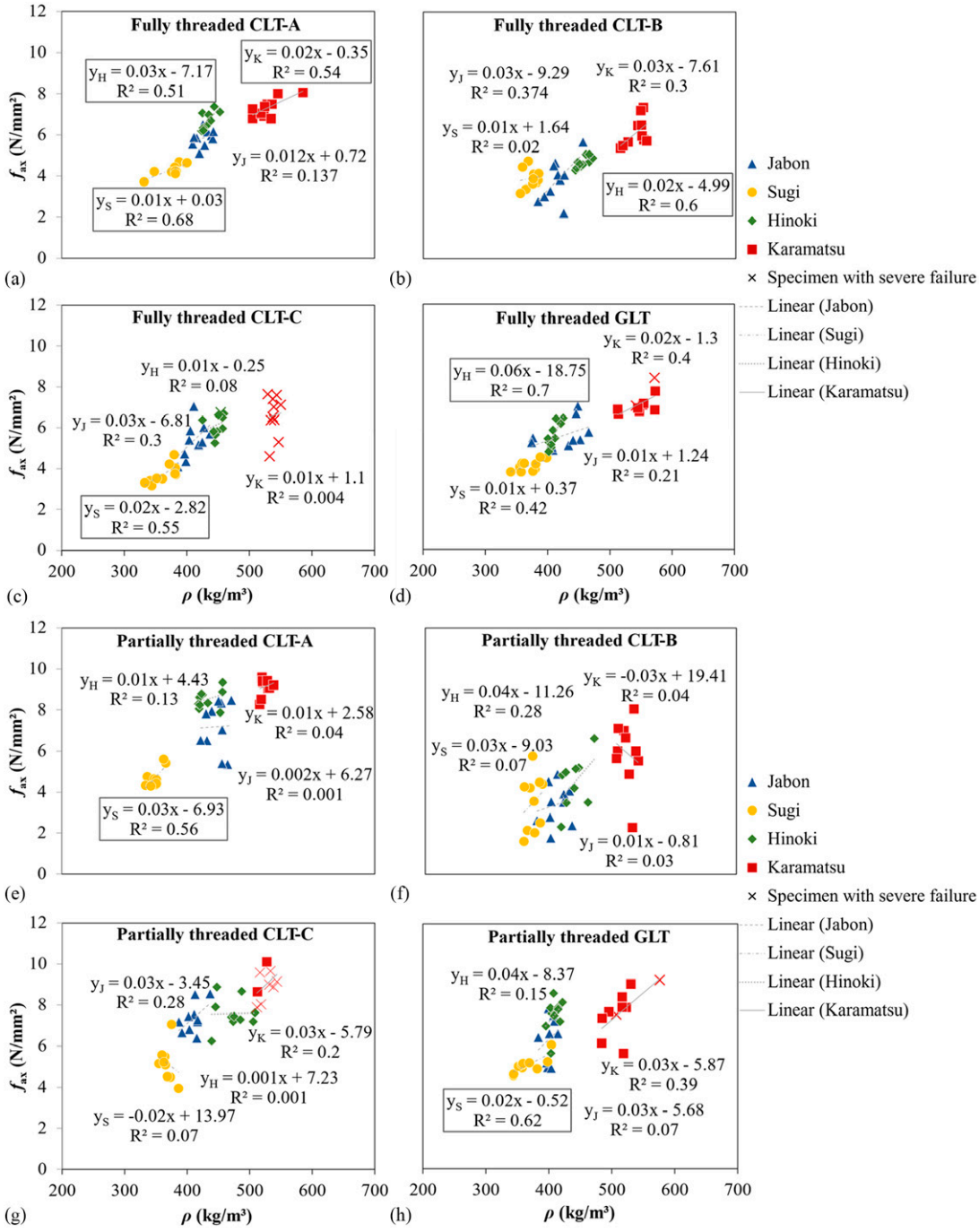

Figure 9. The linear regression graphics analysis of the withdrawal strength depends on the lamina density: (a)-(d) specimens with fully threaded STS and (e)-(h) specimens with partially threaded self-tapping screw.

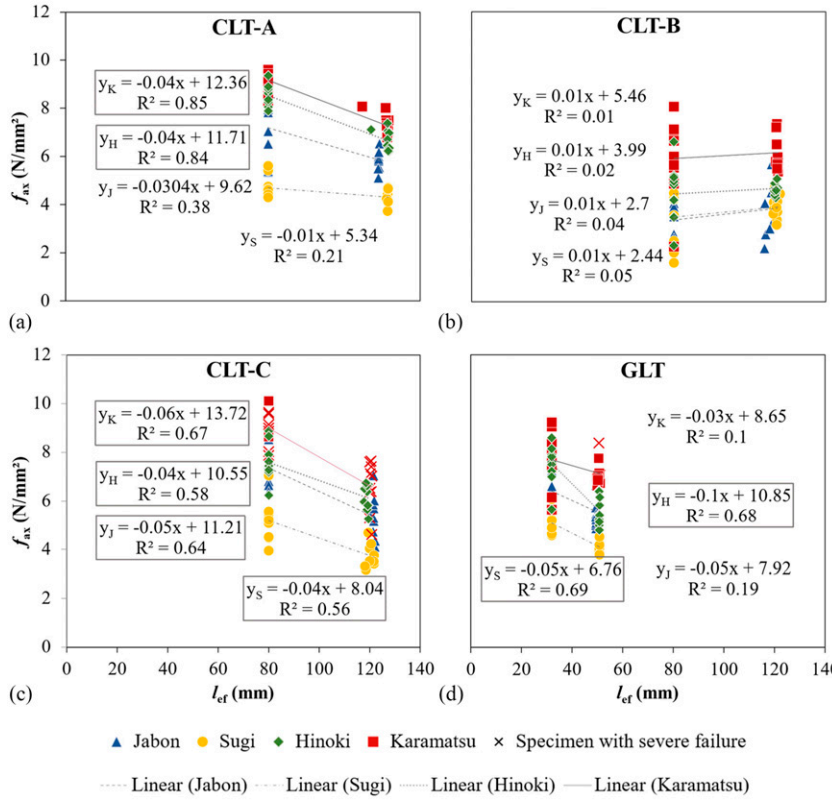

Figure 10. The linear regression graphics analysis of the withdrawal strength depends on the effective insertion length of the self-tapping screw threaded part.

perpendicular to the grain of CLT karamatsu in the first layer. Severe failures were also found on some dense GLT specimens. This would be the important case for the spacing method of STS installment on the narrow edge of the dense wood material in the tangential direction and the dense unidirectional layup material and solid wood in the radial direction. This also proved that the cross-lamination method might enhance the prevention of severe failures.

Figure 11. Typical withdrawal failure mode.

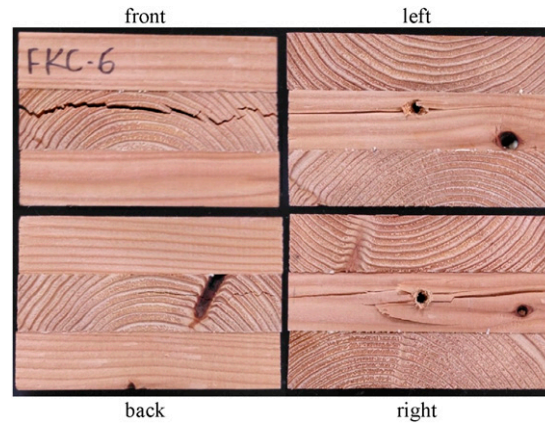

Figure 12. Typical crack failure mode.

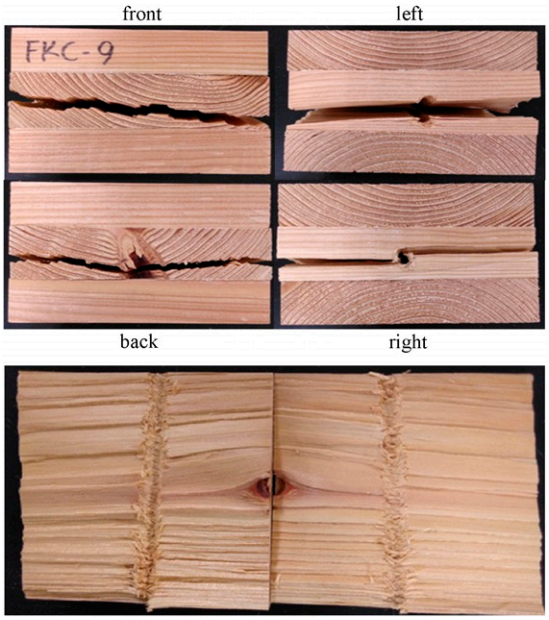

Figure 13. Typical split failure.

CONCLUSIONS

Prior to assessing the prospect of the jabon as a fast-growing-tree species for structural purposes, the preliminary test of the lamina material was performed and proved that the bending Young's modulus E_b passed the minimum grade according to the lamina classification in JAS 3079-2013. Within the density (ρ) and the effective insertion length of the threaded part of STS (l_{ef}) bandwidth in this study, the withdrawal strength of fully threaded and partially threaded STS inserted into the different sides of CLT as well as GLT made of jabon, sugi, hinoki, and karamatsu lamina was evaluated. The result showed that the withdrawal strength of the partially threaded STS was higher than that of fully threaded STS concerning the l_{ef} if it was inserted perpendicular to the grain yet was not the pattern in the STS inserted parallel to the grain of the specimen with respect to the differences on stress distribution along the STS. The compatibility of the probabilistic model given in EN 1995-1-1:2004/A1 (2008) on predicting the withdrawal strength with the limited parameters bandwidth in this study was evaluated. It was found that this probabilistic model was suitable for predicting the withdrawal strength of the STS as long as the predicted values underestimated the experimental results. The significant influence of the lamina density was not found in every wood species and the insertion point of the STS due to the unspecific measurement of density on the STS-inserted wood member. The effective insertion length of the STS threaded part seemed to influence the withdrawal strength if it was inserted in the tangential direction of the wood member. According to the observed failure modes, the spacing design of STS installment on the solid (core layer) and unidirectional layups of dense wood members perpendicular to the grain need to be considered to prevent severe failure caused by the withdrawal force.

ACKNOWLEDGMENTS

The brief results of this experiment have been presented in an online poster presentation at the 71st Japan Wood Society Conference, March 2021. In the preparation of the experiment, the authors were assisted by Tomoki Shinohara, a second year master student in a fiscal year 2020.

CONFLICT OF INTEREST

The authors declare that they have no potential conflict of interest that could have influenced the works reported in this paper.

REFERENCES

AIJ (Architectural Institute of Japan) (2006) Standard for Structural Design of Timber Structure (in Japanese). Page 153. Tokyo: Architectural Institute of Japan.

Brandner R (2019) Properties of axially loaded self-tapping screws with focus on application in hardwood. Wood Mater Sci Eng 14(6):254-268, doi: 10.1080/17480272.2019.1635204.

Brandner R, Ringhofer A, Grabner M (2018) Probabilistic models for the withdrawal behavior of single self-tapping screws in the narrow face of cross laminated timber (CLT). Eur J Wood Prod 76:13-30.

Claus T, Seim W, Küllmer J (2022) Force distribution in self-tapping screws: Experimental investigations with fibre Bragg grating measurement screws. Eur J Wood Prod 80:183-197.

Dietsch P, Brandner R (2015) Self-tapping screws and threaded rods as reinforcement for structural timber

elements—A state-of-the-art report. Constr Build Mater 97:78-89, doi: 10.1016/j.conbuildmat.2015.04.028.

EN 338 (2016) Structural timber - Strength classes. Page 7. European Committee for Standardization (CEN). Brussels, Belgium.

EN 1194 (1999) Timber structures—Glued laminated timber. Strength classes and determination of characteristic values. Page 7. European Committee for Standardization (CEN). Brussels, Belgium.

EN 1382 (1999) Timber structures—Test methods: Withdrawal capacity of timber fasteners. Pages 8-9. European Committee for Standardization (CEN), Brussels, Belgium.

EN 1995-1-1 (2004) Eurocode 5: Design of timber structures—Part 1-1: General—Common rules and rules for buildings. Pages 77-78. European Committee for Standardization (CEN), Brussels, Belgium.

EN 1995-1-1:2004/A1 (2008) Eurocode 5: Design of timber structures—Part 1-1: General—Common rules and rules for buildings. Pages 12-13. European Committee for Standardization (CEN), Brussels, Belgium.

Goto Y, Jockwer R, Kobayashi K, Karube Y, Fukuyama H (2018) Legislative background and building culture for the design of timber structures in Europe and Japan. Pages 8-9 *in* Proceedings, World Conference on Timber Engineering (WCTE 2018), Seoul, Republic of Korea.

Izzi M, Casagrande D, Bezzi S, Pasca D, Follesa M, Tomasi R (2018) Seismic behaviour of cross-laminated timber structures: A state-of-the-art review. Eng Struct 170:42-52.

JIS Z 2101 (2009) Methods of test for woods. Japanese Industrial Standard.

Kobayashi K (2015) Present and future tasks for screw joints in timber structures. Mokuzai Gakkaishi 61(3): 162-168.

Krisnawati H, Kallio M, Kanninen M (2011) *Anthocephalus cadamba Miq.: Ekologi, Silvikultur dan Produktivitas* [*Anthocephalus cadamba Miq.*: Ecology, Silviculture dan Produktivity]. Center for International Forestry Research, Bogor, Indonesia.

Mahdavifar V, Sinha A, Barbosa A R, Muszynski L, Gupta R (2018) Lateral and withdrawal capacity of fasteners on hybrid cross-laminated timber panels. J Mater Civ Eng, 30(9):1-11.

Mansur I, Tuheteru FD (2010) *Kayu Jabon* [Jabon Wood]. Penebar Swadaya, Jakarta.

Mohammad M, Douglas B, Rammer D, Pryor SE (2013) Chapter 5—Connections in cross-laminated timber buildings. Pages 3-44 *in* E Karacabeyli and B Douglas, eds. CLT handbook: Cross-laminated timber. FPInnovations, Pointe-Claire, QC, Canada.

Okuda S, Corpataux L, Muthukrishnan S, Wei KH (2018) Cross-laminated timber with renewable, fast-growing tropical species in Southeast Asia. Pages 1-2 *in* Proceedings, World Conference on Timber Engineering (WCTE 2018), Seoul, Republic of Korea.

Pang S-J, Ahn K-S, Kang SG, Oh J-K (2020) Prediction of withdrawal resistance for a screw in hybrid cross-laminated timber. J Wood Sci 66(79):1-11.

Passarelli RN, Koshihara M (2018) The implementation of Japanese CLT: Current situation and future tasks. *in* Proceedings, World Conference on Timber Engineering (WCTE 2018), Seoul, Republic of Korea.

Ringhofer A, Brandner R, Schickhofer G (2015) Withdrawal resistance of self-tapping screws in unidirectional and orthogonal layered timber products. Mater Struct 48: 1435-1447, doi: 10.1617/s11527-013-0244-9.

Uibel T, Blaß HJ (2007) Edge Joints with Dowel Type Fasteners in Cross Laminated Timber. Pages 6-11 *in* Proceedings, International Council for Research and Innovation in Building and Construction Working Commission W18 - Timber Structures (CIB-W18/40-7-2), Bled, Slovenia.

Uibel T, Blaß HJ (2013). Joints with Dowel type fasteners in CLT structures. Pages 119-134 *in* Proceedings, European Conference on Cross Laminated Timber, Graz, Austria.

Xu J, Zhang S, Wu G, Gong Y, Ren H (2021) Withdrawal properties of self-tapping screws in Japanese larch (*Larix kaempferi* (Lamb.) Carr.) cross laminated timber. Forests 12(524):1-13.